



Influence of Electrochemical Etching on Electroluminescence from n-Type 4H- and 6H-SiC

D. H. van Dorp,^z J. H. den Otter, N. Hijnen, M. Bergmeijer, and J. J. Kelly*

Condensed Matter and Interfaces, Debye Institute for NanoMaterials Science, Utrecht University, 3584 CC Utrecht, The Netherlands

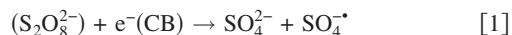
The influence of electrochemical etching on the electroluminescence properties of n-type 6H- and 4H-SiC was investigated. Luminescence was generated by forward-biasing the semiconductor in an electrolyte solution containing a hole-injecting species. The emission properties of unetched, uniformly etched, and porous-etched substrates are compared. It is shown that the spectral distribution of the luminescence and the emission intensity strongly depends on photoanodic treatment.
 © 2009 The Electrochemical Society. [DOI: 10.1149/1.3115404] All rights reserved.

Manuscript submitted February 3, 2009; revised manuscript received March 16, 2009. Published April 8, 2009.

The first commercially available blue light-emitting diode was based on SiC and introduced by Cree in 1989. It was subsequently made redundant by group III nitride-based devices.¹ SiC is still used in UV photodetection.²⁻⁴ In such electronic applications, recombination at defects in the bandgap determines the optical properties. A defect-free material is important for electronic devices. Defects may be introduced during crystal growth or by polishing (mechanical or chemomechanical), sputter etching,^{5,6} or handling. Luminescence measurements give information about defects in semiconductors. Chemical and electrochemical etching can be used to remove damaged layers and modify the surface chemistry, thereby influencing radiative recombination.

In this paper we describe the use of forward-biased n-type 4H- and 6H-SiC electrodes in a solution containing a hole-injecting species, the peroxydisulphate ($S_2O_8^{2-}$) anion, to generate electroluminescence (EL) to study the influence of electrochemical etching of the semiconductor on the light emission. We show that (uniform) photoanodic etching of as-received wafers in KOH solution changes the spectral distribution of the emitted light quite radically. Photoanodic etching in acidic fluoride solution gives rise to porosity, which markedly enhances the EL emission. We describe characteristic luminescence from n-type SiC during porous etching in the dark under breakdown conditions. Matsumoto et al.,⁷ Petrovakoč et al.,⁸ and Kim et al.⁹ reported a strong enhancement of the room-temperature photoluminescence from porous n-type 6H-SiC. Kim et al. also noted an increase in emitted intensity for EL.

EL from n-type SiC electrodes was first reported by Manivannan et al.¹⁰⁻¹³ They used the peroxydisulphate anion ($S_2O_8^{2-}$) to “inject” holes into the valence band (VB) of the semiconductor. At negative potentials corresponding to majority carrier accumulation, the reaction occurs by a two-step process. The ($S_2O_8^{2-}$) anion captures an electron from the conduction band (CB) of the semiconductor



The $SO_4^{\cdot-}$ radical anion is an extremely strong electron acceptor and picks up an electron from the VB, i.e., it generates a hole



The radiative recombination of the hole with an electron, either directly or via bandgap states, gives rise to EL.

Experimental

We used single-crystal nitrogen-doped 4H- and 6H-SiC wafers (research grade, Si polar face) from Cree with a resistivity in the range 0.06–0.07 Ω cm. The wafers were contacted with a 300 nm Ti/Au layer annealed in a 1 s step at 1000°C. The samples were mounted as a rotating disk electrode (RDE). Measurements were

performed in a conventional three-electrode cell with a platinum counter electrode and a saturated calomel electrode (SCE) as a reference. The light source for photoanodic etching was a 500 W Hg arc lamp (Oriol 66941). UV light from the beam was directed onto the sample using a dichroic mirror (280–400 nm).¹⁴ For the EL measurements, freshly made solutions containing 0.1 M $K_2S_2O_8$ + 0.5 M H_2SO_4 were prepared. The optical fiber connected to the charge-coupled device camera (Acton Research Corporation, Spectra Pro-300i) was positioned 1 cm above the stationary electrode. The spectra were recorded 1 s after the potential was applied. Before each measurement, the surface oxide was removed by dipping in 1 M HF solution. The integration time of the recorded spectra was 10 s. The EL measurements were in all cases stable in time; when 10 subsequent spectra were recorded at a given potential, the peak intensities varied by about 10%.

Results and Discussion

Electrochemistry.—As a prelude to the EL study, we first looked at the kinetics of the $S_2O_8^{2-}$ reduction (Eq. 1 and 2) at SiC. Figure 1 shows current-potential curves for an n-type porous 6H-SiC RDE in 0.1 M $S_2O_8^{2-}$ /0.5 M H_2SO_4 solution. For comparison, the corresponding curve for a $S_2O_8^{2-}$ -free H_2SO_4 solution (solid curve) is also given. In a $S_2O_8^{2-}$ -free H_2SO_4 solution the electrochemical reaction occurring is the proton reduction to give hydrogen gas [$2H^+ + 2e^- \rightarrow H_2(g)$]. The flatband potential (U_{FB}) of n-type 6H-SiC in H_2SO_4 solution is at -1.0 V vs SCE.¹⁵ At a more negative potential, majority carriers “accumulate” at the electrode surface. The Fermi

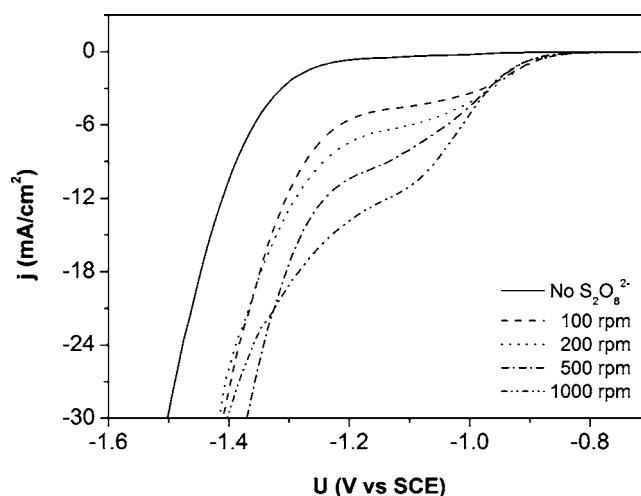


Figure 1. Influence of rotation rate on the cathodic reduction of $S_2O_8^{2-}$ for a porous n-type 6H-SiC electrode in 0.1 M $S_2O_8^{2-}$ /0.5 M H_2SO_4 solution. The reduction of protons in 0.5 M H_2SO_4 is indicated by the solid line.

* Electrochemical Society Active Member.

^z E-mail: d.h.vandorp@uu.nl

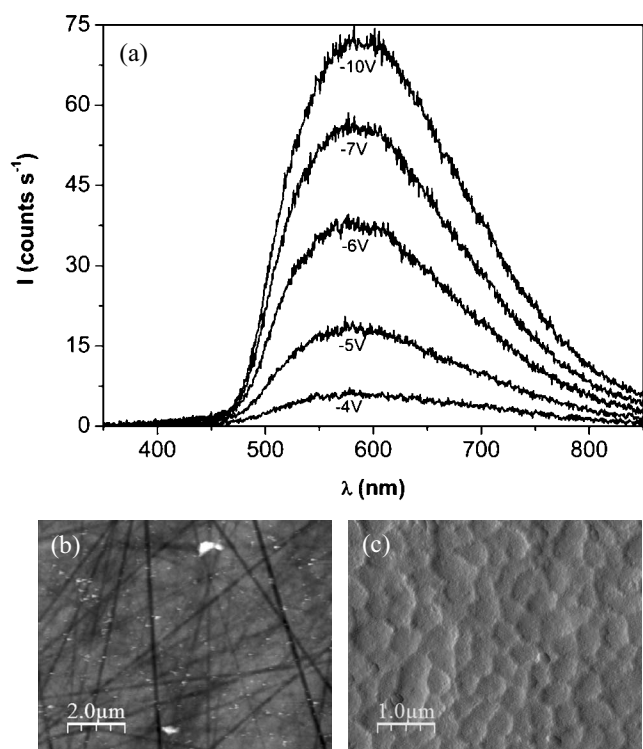


Figure 2. (a) EL spectra of an unetched n-type 6H-SiC wafer at various potentials (vs SCE) in 0.1 M $\text{S}_2\text{O}_8^{2-}/0.5$ M H_2SO_4 solution. AFM images of the surface of (b) an as-received wafer and (c) after uniform etching in KOH solution.

level becomes pinned and the applied potential drops over the Helmholtz layer in the solution. A considerable overpotential is required to generate hydrogen: the onset potential is at -1.2 V. $\text{S}_2\text{O}_8^{2-}$ reduction begins before U_{FB} (at -0.9 V); clearly this reaction is kinetically favorable. A plateau in the current-potential curve indicates a mass-transport limitation of the $\text{S}_2\text{O}_8^{2-}$ reduction. This is confirmed by the increase in plateau current with increasing electrode rotation rate. One can expect the hydrogen gas evolution at a negative potential to influence the hydrodynamics of the system, especially for a stationary electrode.

EL after photoanodic etching.—Light emission is observed for “as-received” wafers (not etched) at potentials ≤ -2 V and the intensity increases with increasing polarization up to -10 V (Fig. 2). The EL spectra show a broad defect emission band which rises steeply at about 475 nm, peaks at about 590 nm (2.10 eV), and has a long tail extending into the near infrared. This spectrum resembles that of the EL of n-type SiC reported by Manivannan et al.,¹² who suggested that the broad emission was related to donor-acceptor recombination. High concentrations of aluminum (up to 0.34 atom %) were found using X-ray fluorescence spectrometry in their nitrogen-doped SiC.¹⁰ Impurity levels in our wafers are below the secondary-ion mass spectrometry detection limit. It is therefore unlikely that donor-acceptor emission is important. The emission intensity is low and no (near) bandgap emission is observed; this may be related to a high density of nonradiative recombination centers arising from (chemo)mechanical polishing or handling of the wafer, which causes damage at the surface and is revealed as scratches by an atomic force microscope (AFM) (see inset of Fig. 2).

Surface damage can be removed by electrochemical etching in KOH solution. Figure 2c shows an AFM image of an etched surface. Scratches are no longer visible; the surface shows microroughness.^{16,17} After the removal of a thickness of 10.3 μm of the surface layer, the emission spectrum changed considerably (Fig. 3). The

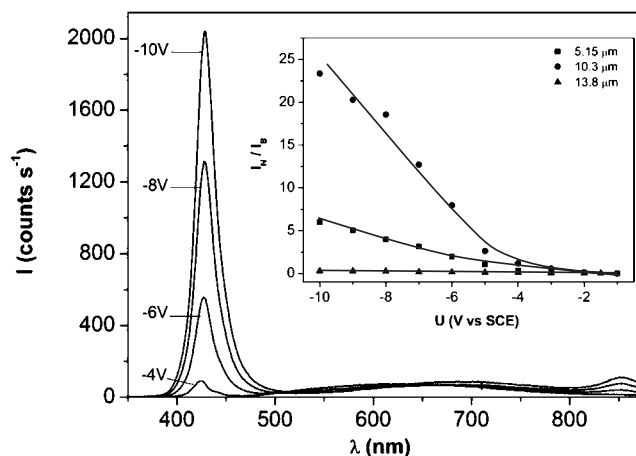


Figure 3. EL spectra of 6H-SiC in 0.1 M $\text{S}_2\text{O}_8^{2-}/0.5$ M H_2SO_4 solution at various potentials after etching in 0.1 M KOH solution (10.3 μm removed). The inset shows the narrow peak/broad peak intensity ratio for three etch depths.

onset of the EL shifts to a positive potential ($U = -1.25$ V). In contrast to the unetched samples, a narrow emission band is observed, which markedly increases with increasing bias. The emission peaks at 424 nm (2.92 eV) and, subsequently, shifts slightly to 428 nm (2.90 eV) at potentials < -5 V. Since the bandgap of 6H-SiC is 3.03 eV (409 nm),¹⁸ the EL is attributed to a donor-VB emission. Our wafers were nitrogen doped, and it is known that the donor resides on a carbon site in the SiC crystal.¹⁸ In 6H-SiC, nitrogen atoms can occupy a hexagonal (h) site or two different cubic (k_1 , k_2) sites. Hall measurements revealed two donor levels with ionization energies of 85 and 125 meV for the h site and k_1 , k_2 sites, respectively. The ground-state energy difference between k_1 and k_2 could not be resolved. The ratio of the density of h and k_1 , k_2 lattice sites is 1:2.¹⁹ Transitions from the nitrogen donor to the VB would therefore account for emission at approximately 2.94 eV (h) and 2.90 eV (k_1 , k_2). At potentials < -5 V the emission from the h site apparently saturates and the emission from the k_1 , k_2 site is favored. The redshift of the narrow emission is accompanied by the occurrence of a small emission peak at 850 nm (1.46 eV), which is attributed to an intrinsic defect.²⁰

The narrow high energy emission appeared when at least 3.5 μm of the surface layer had been removed. The inset of Fig. 3 shows that the narrow peak/broad peak intensity ratio (I_N/I_B) depends on etch depth. The I_N/I_B ratio first increases (5.15, 10.3 μm) but then decreases markedly (13.8 μm); it recovers at a larger depth (not shown). The intensity of the broad emission is almost independent of the etch depth, saturates at lower potentials, and is comparable to that of the unetched sample at a strong bias. The influence of etching becomes clearest for the narrow emission band at potentials below -3 V. I_N/I_B ratios up to 25 have been observed. Comparable results were obtained for the 4H-SiC substrates after photoelectrochemical etching in a KOH solution.

These results suggest a competition between radiative and non-radiative centers for the injected holes. In the unetched sample the broad emission is more efficient than the narrow emission (see Fig. 2). The increase in intensity of the broad EL band with decreasing potential is due to two effects. Convection caused by hydrogen evolution will enhance the diffusion-limited rate of the $\text{S}_2\text{O}_8^{2-}$ reduction reaction (Eq. 1), thus increasing the rate of hole injection. This is supported by the observation that enhanced convection by the mechanical stirring of the solution leads to an emission intensity increase by a factor of 2. Hydrogen can change the surface chemistry or be absorbed in the semiconductor; this may suppress nonradiative recombination. Photoanodic etching is expected to remove surface and subsurface damages while exposing deeper regions of the semi-

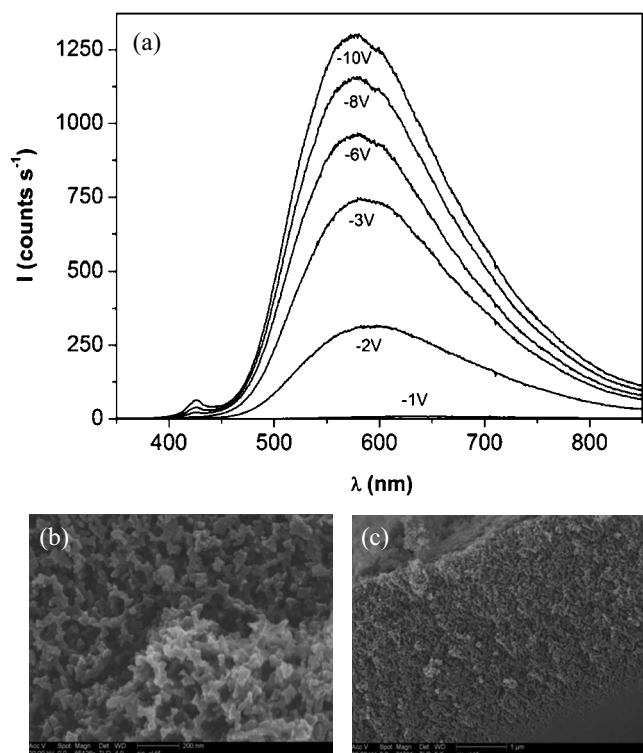


Figure 4. (a) EL spectra at various potentials for porous n-type 6H-SiC in 0.1 M $\text{S}_2\text{O}_8^{2-}$ /0.5 M H_2SO_4 solution. The thickness of the porous layer was approximately 11 μm . Scanning electron microscope images of a porous-etched SiC electrode taken from (b) the top and (c) the side of the layer are shown.

conductor. The broad emission saturates at low potential, enabling the narrow-band emission to be observed (Fig. 3). (This very likely also holds for the 850 nm emission.) The saturation of the h site allows the emission from the k_1 , k_2 lattice site. Here again we see the favorable influence of the potential on the luminescence. This is unusual. For most semiconductors, a negative polarization of the electrode and the hydrogen evolution tend to degrade the surface, enhance surface recombination, and quench luminescence.^{21,22} The unusual chemical stability of SiC is very likely responsible for this difference. The strong dependence of the I_N/I_B ratio on etch depth to large depths indicates that (sub-)surface recombination cannot be (solely) responsible for the results shown in the inset of Fig. 3. We conclude that the recombination dynamics is dependent on position: the density of nonradiative recombination centers is possibly not uniform throughout the crystal.

When n-type SiC is photoanodically etched in HF solution at a moderate light intensity, the semiconductor becomes macroporous.²³⁻²⁵ The EL spectra of an 11 μm thick porous SiC layer are shown in Fig. 4. The broad emission, similar to that observed for the unetched sample, is dominant. The intensity of the broad emission is about 20 times higher than that of unetched or KOH-etched substrates and is clearly visible to the naked eye. The narrow emission at 424 nm appears below $U \leq -3$ V and is much less pronounced than from SiC uniformly etched to 10 μm . No clear correlation was observed between the thickness of the porous layer and the I_N/I_B ratio for samples with an etched depth between 1 and 11 μm . Scattering and absorption of emitted light in the porous layer can therefore be excluded.²⁶ The substantial increase in luminescence intensity is attributed to the much larger surface area of the porous electrode in contact with the electrolyte solution, leading to an increase in the flux of injected holes.

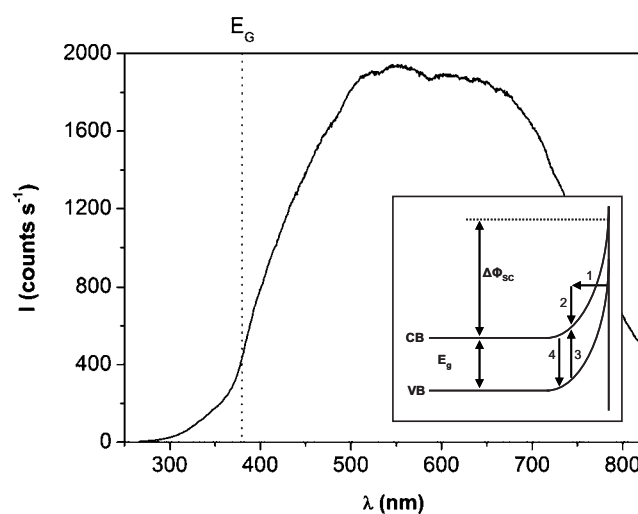


Figure 5. Luminescence spectrum recorded for n-type 4H-SiC in 0.5 M HF solution during porous etching at 14 V. The inset shows a model for impact ionization.

EL under breakdown conditions.—When n-type SiC is etched in an acidic fluoride solution in the dark, i.e., under a strong reverse bias, the semiconductor also becomes porous.^{8,27,28} We have observed that porosification is accompanied by light emission visible to the naked eye. A typical spectrum recorded at 14 V for 4H-SiC is shown in Fig. 5. The emission is completely different from photoluminescence or conventional EL. A broad band is observed over a wide spectral range. Quite remarkably, a significant fraction of emitted light has an energy close to and larger than the indirect bandgap, as indicated by the dotted line. The process responsible for light emission is very likely impact ionization and was also shown for reverse-biased n-type GaP electrodes.²⁹ At a strong band bending, empty states from the CB overlap with filled states at the top of the VB at the surface. As a result, electrons can tunnel from the VB to the CB (step 1, Fig. 4a inset). Electrons injected into the CB are accelerated to the bulk by the high electric field of the depletion layer, and the holes are used for porous etching. If the electron can gain sufficient energy (depending on the band structure),³⁰ it can excite a VB electron over the bandgap via a collision process (steps 2 and 3). Some carriers are further heated by the strong field, while other pairs recombine radiatively (step 4). The supra-bandgap emission is possible due to the population of the higher energy CB valleys as a result of the strong electric field.³⁰

Light emission is observed for potentials ≥ 6 V. The integrated emission intensity increases with potential and peaks at 14 V, after which it decreases and becomes almost zero. This sudden decrease in intensity coincides with a strong increase in current (not shown). The latter is due to the oxidation of water by VB holes and is accompanied by a severe gas formation. It is likely that the porous layer is damaged during this process.

When n-type SiC is etched in KOH solution in the dark, spectra comparable to those obtained for porous etching in HF solution in the dark (not shown) are obtained. The potential at which light emission is observed is, however, much more positive than for porous SiC ($U \geq 23$ V). This suggests that in porous SiC, as in porous GaP,²⁹ the enhancement of the electric field at the pore tips is responsible for current flow and light emission.³¹

Conclusions

We have shown that EL from the n-type SiC/ $\text{S}_2\text{O}_8^{2-}$ solution diode is sensitive to the electrochemical pretreatment of the electrode and to the applied potential. The spectral distribution of the luminescence and the intensity of the two main emission bands are influenced by photoanodic treatment, i.e., uniform etching in KOH

solution and porous etching in HF solution. This relatively simple approach, combining anodic etching and in situ EL, might be interesting for applications such as quality control of SiC wafers.

Acknowledgments

The authors thank Hans Ligthart and Rinus Mackaay for contributing to this work. This work was financially supported by the Dutch Technology Foundation (STW, no. UPC-6317).

Utrecht University assisted in meeting the publication costs of this article.

References

1. S. Nakamura, S. Pearton, and G. Fasol, *The Blue Laser Diode*, 2nd ed., Springer, New York (2000).
2. X. P. Chen, H. L. Zhu, J. F. Cai, and Z. Y. Wua, *J. Appl. Phys.*, **102**, 024505 (2007).
3. Z. Wu, X. Xin, F. Yan, and J. H. Zhao, *Mater. Sci. Forum*, **457–460**, 1491 (2004).
4. V. I. Sankin and V. P. Chelibanov, *Phys. Status Solidi A*, **185**, 153 (2001).
5. N. M. Stanton, A. J. Kent, P. Hawker, T. S. Cheng, C. T. Foxon, D. Korakakis, R. P. Campion, C. R. Staddon, and J. R. Middleton, *Mater. Sci. Eng., B*, **68**, 52 (1999).
6. J. Skriniarova, P. Bochem, A. Fox, and P. Kordos, *J. Vac. Sci. Technol. B*, **19**, 1721 (2001).
7. T. Matsumoto, J. Takahashi, T. Tamaki, T. Futagi, H. Mimura, and Y. Kanemitsu, *Appl. Phys. Lett.*, **64**, 226 (1994).
8. V. Petrovakocho, O. Sreseli, G. Polisski, D. Kovalev, T. Muschik, and F. Koch, *Thin Solid Films*, **255**, 107 (1995).
9. S. Kim, J. E. Spanier, and I. P. Herman, *Jpn. J. Appl. Phys., Part 1*, **39**, 5875 (2000).
10. A. Manivannan, K. Hashimoto, and A. Fujishima, *J. Phys. Chem.*, **96**, 3766 (1992).
11. A. Manivannan, K. Hashimoto, T. Sakata, and A. Fujishima, *J. Phys. Chem.*, **96**, 7399 (1992).
12. A. Manivannan, K. Itoh, K. Hashimoto, T. Sakata, and A. Fujishima, *J. Electrochem. Soc.*, **137**, 3121 (1990).
13. A. Manivannan and A. Fujishima, *J. Lumin.*, **42**, 43 (1988).
14. D. H. van Dorp, Ph.D. Thesis, Utrecht University (2008).
15. J. van de Lagemaat, D. Vanmaekelbergh, and J. J. Kelly, *J. Appl. Phys.*, **83**, 6089 (1998).
16. D. H. van Dorp and J. J. Kelly, *J. Electroanal. Chem.*, **599**, 260 (2007).
17. D. H. van Dorp, J. L. Weyher, and J. J. Kelly, *J. Micromech. Microeng.*, **17**, S50 (2007).
18. G. L. Harris, *Properties of SiC*, INSPEC, London (1995).
19. W. Suttrop, G. Pensl, W. J. Choyke, R. Stein, and S. Leibenzeder, *J. Appl. Phys.*, **72**, 3708 (1992).
20. N. I. Kuznetsov and J. A. Edmond, *Semiconductors*, **31**, 1049 (1997).
21. G. H. Schoenmakers, E. Bakkers, and J. J. Kelly, *J. Electrochem. Soc.*, **144**, 2329 (1997).
22. B. Smandek and H. Gerischer, *Electrochim. Acta*, **30**, 1101 (1985).
23. D. H. van Dorp, J. J. H. B. Sattler, J. H. den Otter, and J. J. Kelly, *Electrochim. Acta*, Submitted.
24. J. S. Shor, I. Grimberg, B. Z. Weiss, and A. D. Kurtz, *Appl. Phys. Lett.*, **62**, 2836 (1993).
25. J. S. Shor and A. D. Kurtz, *J. Electrochem. Soc.*, **141**, 778 (1994).
26. A. F. van Driel, D. Vanmaekelbergh, and J. J. Kelly, *Appl. Phys. Lett.*, **84**, 3852 (2004).
27. S. Zangoie and H. Arwin, *J. Electrochem. Soc.*, **148**, G297 (2001).
28. S. Zangoie and H. Arwin, *Phys. Status Solidi A*, **182**, 213 (2000).
29. A. F. van Driel, B. P. J. Bret, D. Vanmaekelbergh, and J. J. Kelly, *Surf. Sci.*, **529**, 197 (2003).
30. S. M. Sze, *Physics of Semiconductor Devices*, John Wiley & Sons, New York (1981).
31. X. G. Zhang, *J. Electrochem. Soc.*, **138**, 3750 (1991).